

## Non-isothermal kinetic characterisation of a gas–solid reaction by TG analysis

ŽELJKO ČUPIĆ<sup>\*#</sup>, DUŠAN JOVANOVIĆ,<sup>1</sup> JUGOSLAV KRSTIĆ<sup>1#</sup>, NIKOLA VUKELIĆ<sup>2</sup> and  
ZORAN NEDIĆ<sup>2#</sup>

<sup>1</sup>Institute of Chemistry, Technology and Metallurgy, Center of Catalysis and Chemical Engineering,  
Njegoševa 12, 11000 Belgrade, (e-mail: zcupic@nanosys.ihtm.bg.ac.yu) and <sup>2</sup>Faculty for Physical  
Chemistry, University of Belgrade, P. O. Box 137, 11001 Belgrade, Serbia and Montenegro

(Received 9 July 2004)

*Abstract:* A series of silica-supported Ni-catalyst precursors was synthesized, with different SiO<sub>2</sub>/Ni mole ratios between 0.2 and 1.15. The reduction of all the prepared samples was studied by thermogravimetry (TG) in a hydrogen flow. The results of the TG analysis were analyzed by the multi-thermal history model-fitting method, with non-linear regression. The activation energies for the reduction of each sample were determined. The statistical F-test was performed to discriminate between various models. It was found that increasing the SiO<sub>2</sub>/Ni mole ratio leads to a change in the reaction mechanism of the nickel reduction, resulting finally in a change from second order reaction kinetics to three halves order reaction kinetics.

*Keywords:* non-isothermal kinetics, thermogravimetry, non-linear regression, nickel catalyst, catalyst preparation.

### INTRODUCTION

#### *Reduction of supported-Ni in a hydrogen atmosphere*

The reduction of Ni in a hydrogen atmosphere is an important step in the synthesis of frequently used Ni hydrogenation catalysts. The synthesis usually involves impregnation or precipitation of a Ni salt on the chosen support, followed by calcination, reduction and passivation. It was reported previously that good hydrogenation catalysts could be obtained if Ni(NO<sub>3</sub>)<sub>2</sub> is precipitated with Na<sub>2</sub>CO<sub>3</sub> onto a SiO<sub>2</sub> support (activated diatomite), with subsequent reduction in hydrogen and passivation in hydrogenation fat (calcination excluded).<sup>1</sup>

The possibilities for the characterization of the reduced catalysts is limited by their pyrophoric properties. Hence, after reduction, the catalyst must be passivated before any further manipulation. On the other hand, the precursor properties could

\* Author for correspondence.

# Serbian Chemical Society active member.

be significantly changed during the reduction process, and the properties of the final catalyst are strongly dependent on the reduction conditions.

More generally the properties of the final catalyst, such as catalytic activity, selectivity *etc.*, are strongly dependent on various process parameters used in the preparation treatment.<sup>2,3</sup> When a nickel solution is treated with sodium carbonate, basic nickel carbonate  $\text{NiCO}_3 \cdot x\text{Ni}(\text{OH})_2 \cdot y\text{H}_2\text{O}$  is formed. The stoichiometric composition of the resulting precipitate varies with the reaction conditions. The resulting material decomposes slowly in an inert atmosphere, from 220 °C up to 850 °C, but nearly complete transformation occurs between 300 °C and 350 °C.<sup>4</sup> Several authors agreed that the thermal decomposition of the basic nickel carbonate to NiO proceeds in two steps, *i.e.*, the evolution of the crystal water in the first step and the evolution of  $\text{H}_2\text{O}$  and  $\text{CO}_2$  in the second step.<sup>5,6</sup>

The formation of nickel phyllosilicate during the deposition – precipitation procedure was systematically studied by P. Burattin *et al.*<sup>7</sup> The authors found that long deposition – precipitation times are favourable for silicate formation, while at short deposition – precipitation times, the hydroxide is favoured, at least with low surface area supports.

Bhering *et al.*<sup>3</sup> use a statistical experimental setup to study the reduction step in the preparation of silica-supported nickel catalysts. These authors differentiated between precursors with weak nickel-support interactions and ones with strong nickel-support interactions. The former should be attained by the predominant formation of NiO during the precipitation, aging and calcination phases, while the latter result when nickel silicate is formed. Short ageing time and high Ni loading are favourable for NiO formation. The weak interaction samples seem to be completely reduced even at low temperatures while the strong interaction samples are reduced to different degrees at different temperatures due to the high temperature stability of nickel silicate. In both cases, the specific area of the final catalyst depends strongly on the flow rate and hydrogen concentration.

Hence, for highly reducible supported Ni precursors, the formation of silicates should be avoided. Therefore, low surface area silica supports and fast precipitation procedures should be used,<sup>1</sup> resulting in supported basic nickel carbonate. However, the mechanism of the supported basic nickel carbonate reduction is not clear, and it is complicated by the fact that reduction occurs in the temperature interval corresponding to the thermal decomposition of basic nickel carbonate. Therefore, the reaction kinetics of the reduction process could give a new insight into the mechanism of the process and lead to improvements of the catalysts.

#### *Kinetics from non-isothermal TG analysis*

Due to their complexity, Ni compounds are very interesting objects for analysis. Furthermore, the significant weight loss occurring during the reduction of Ni compounds makes this system suitable for thermogravimetry (TG) analysis. TG is a conve-

nient technique for studying the kinetics of processes involving solids, such as gas–solid reactions, by following the weight changes of the samples with time.<sup>8</sup>

In TG practice, it is usual to present reaction kinetics by a single-process rate law:

$$\frac{d\alpha}{dt} = k(T)f(\alpha) \quad (1)$$

where  $t$  is time,  $T$  the absolute temperature and  $\alpha$  the degree of conversion:

$$\alpha = \frac{w_0 - w}{w_0 - w_f} \quad (2)$$

where  $w_0$ ,  $w$  and  $w_f$  represent the initial mass, actual mass at temperature  $T$  and final mass of the sample, respectively. The kinetic function  $f(\alpha)$  is related to the reaction mechanism. The kinetic function  $f(\alpha)$  for various useful kinetic models are listed in Table I.<sup>9</sup>

TABLE I. The set of reaction models applied to describe gas–solid reaction kinetics in model-fitting methods

Kinetic model	$f(a)$	$g(a)$	Observations
R2	$(1 - \alpha)^{1/2}$	$2[1 - (1 - \alpha)^{1/2}]$	One-half order kinetics; two dimensional advance of the reaction interface
R3	$(1 - \alpha)^{2/3}$	$3[1 - (1 - \alpha)^{1/3}]$	Two-thirds order kinetics; three dimensional advance of the reaction interface
F1	$1 - \alpha$	$-\ln(1 - \alpha)$	First order kinetics
F3/2	$(1 - \alpha)^{3/2}$	$2[(1 - \alpha)^{1/2} - 1]$	Three halves order kinetics
F2	$(1 - \alpha)^2$	$\alpha/(1 - \alpha)$	Second order kinetics
A2	$(1 - \alpha)[- \ln(1 - \alpha)]^{1/2}$	$2[- \ln(1 - \alpha)]^{1/2}$	Avrami–Yerofeyev equation for $n = 2$
A3	$(1 - \alpha)[- \ln(1 - \alpha)]^{2/3}$	$3[- \ln(1 - \alpha)]^{1/3}$	Avrami–Yerofeyev equation for $n = 3$
A4	$(1 - \alpha)[- \ln(1 - \alpha)]^{3/4}$	$4[- \ln(1 - \alpha)]^{1/4}$	Avrami–Yerofeyev equation for $n = 4$
D3	$(1 - \alpha)^{2/3}/[1 - (1 - \alpha)^{1/3}]$	$3/2[1 - (1 - \alpha)^{1/3}]^2$	Jander equation (3D diffusion)
D5	$(1 - \alpha)^{5/3}/[1 - (1 - \alpha)^{1/3}]$	$3/2[1 - (1 - \alpha)^{-1/3} - 1]^2$	Zhuravlev–Lesokhin–Tempelman equation

The temperature dependence of the reaction constant is normally expressed by the Arrhenius equation:

$$k = A \exp\left(-\frac{E_a}{RT}\right) \quad (3)$$

where  $E_a$  is the activation energy,  $A$  the pre-exponential factor and  $R$  is the gas constant.

For the determination of the so-called kinetic triplet ( $A, E_a, f(\alpha)$ ), the model-fitting methods use the integrated form of Eq. (1):

$$g(\alpha) = \int_0^{\alpha} \frac{d\alpha}{f(\alpha)} = \frac{A}{\beta} \int_{T_0}^T \exp\left(-\frac{E_a}{RT}\right) dT \quad (4)$$

where  $\beta$  is the heating rate and the expression on the right hand side is known as the temperature integral, which must be approximated.

It is possible, and also frequently done, to evaluate the kinetic triplet from a single experiment using the Eq. (4). However, it is now a well-recognized fact<sup>10</sup> that thermal analysis should not be used for the determination of kinetic parameters if only one heating rate was employed. Such a practice leads to wide intervals of the kinetic parameters determined for the same reaction systems, under different conditions. Moreover, Vyazovkin and Wight<sup>11</sup> argued that the model fitting method, when applied to non-isothermal data, results in highly uncertain kinetic triplets.

Therefore, model-free methods, like the isoconversional methods, are used frequently to obtain invariant sets of kinetic parameters.<sup>12, 13</sup> However, by correctly applying multi-thermal history model-fitting methods, it is possible to retrieve correct kinetic triplets.<sup>14</sup>

If the non-linear regression method is combined with model fitting methods, any set of model reactions can be applied. The kinetic Eq. (1) is integrated numerically and the simulated results compared with the experimental ones. An optimization algorithm is then used to find the best set of kinetic parameters according to the largest value of the correlation coefficient.<sup>15</sup> Such a method is generally quite applicable, but it should be noted that imagination in the construction of the model should be limited by known experimental facts.

It is sometimes forgotten that the highest correlation coefficient does not necessarily mean that the best model is chosen. In fact, usually several models give an acceptably good fit. In order to quantitatively evaluate the quality of the fitting of the experimental data obtained with different models, the statistical  $F$ -test is usually used. Therefore, the  $F$  value was calculated as the ratio of the variances:

$$F = \frac{(RSS / f)}{(RSS / f)_{\min}} \quad (5)$$

where  $RSS$  is the residual sum of the squares,  $f$  is the number of degrees of freedom, depending on the number of experimental points, and the subscript min denotes the minimum value of the  $RSS/f$  among the different models.

Only models with an  $F$  value higher than  $F_{95}$  can be discarded as inappropriate with a probability higher than 95 %. Tables could be used, as well as the numerical approximations available<sup>16</sup> for the  $F_{95}$  value.

Moreover, in the determination of kinetic parameters by the application of any of the described methods, due care should be given to the parametric sensitivity.<sup>16</sup>

Hence, the kinetic parameters could be determined only within some uncertainty limits, depending on the local sensitivity of the process dynamics to slight changes in the parameters. The parametric sensitivity can easily be evaluated from the changes of the criteria function (*RSS* for example), caused by a small change in the kinetic parameters of the tested model.

Furthermore, the numerical optimization procedure can be significantly improved if the parameters are normalized.<sup>17</sup> As *A* is normally very much larger than  $E_a$  (Eq. (1)), and because the activation energy appears in the exponent, these parameters exhibit a strong, non-linear correlation when they are fitted to the experimental data. Simple scaling procedure has the double effect of reducing the correlation between *A* and  $E_a$  and reducing the non-linearity of the correlation. Therefore, the rate constant could be rewritten in the form:

$$k = A \exp\left(-\frac{E_a}{RT}\right) = \left( A \exp\left(-\frac{E_a}{RT_0}\right) \right) \exp\left(-\frac{E_a}{R} \left(\frac{1}{T} - \frac{1}{T_0}\right)\right) \quad (6)$$

where  $T_0$  is a temperature near the middle of the studied temperature range. The described scaling procedure is called temperature centering. Hence, the numerical least-squares procedures used to estimate the fit of the parameters will be more robust.

#### EXPERIMENTAL

A series of Ni catalyst precursors was synthesized with different SiO<sub>2</sub>/Ni mole ratio values between 0.2 and 1.15 by a literature procedure.<sup>1</sup> The nickel ions and promotor's ions (Mg) were precipitated at an elevated temperature (90 °C) with a strictly defined pH value (pH 9.2), from a solution of Ni(NO<sub>3</sub>)<sub>2</sub> and Mg(NO<sub>3</sub>)<sub>2</sub> (mole ratio Mg/Ni = 0.1) using Na<sub>2</sub>CO<sub>3</sub> as the alkaline agent. An activated domestic diatomite with a low surface area was added to the reaction mixture as a support. Upon completion of the precipitation process, the filtered and rinsed precipitate was transferred to an oven and dried at a temperature of 120 – 140 °C.

The reduction of all the prepared samples was studied by thermogravimetry (Linesies System 2000) at different heating rates between 2 and 20 degrees/min, in a hydrogen flow. The catalytic activity of the samples in hydrogenation of the soybean oil was tested earlier.<sup>1</sup> A decrease of the activity was observed with increasing heating rate during the reduction step of the synthesis procedure.

#### RESULTS AND DISCUSSION

The results of the TG analysis are shown in Fig. 1. Only part of the TG curves is presented, corresponding to the reduction process. At lower temperatures (< 150 °C) almost constant weight loss was observed for all samples (13 – 15 %), corresponding to the loss of sorbed water. Therefore, in Fig. 1, and subsequently, the relative weight loss, referring to the sample mass at the beginning of the reduction process, is used.

From the results given in Fig. 1, it can be seen that the starting temperature of the reduction process depended on the heating rate and not on the SiO<sub>2</sub>/Ni mole ratio (Fig. 2).

On the other hand, the final weight loss depended on the  $\text{SiO}_2/\text{Ni}$  mole ratio and not on the heating rate (Table II), indicating that complete hydrogenation of all samples was achieved. Further, assuming that complete hydrogenation was achieved, the composition of the precursor samples was calculated from the final mass loss. The difference in the composition of the precursor samples probably originated from the synthesis procedure and conditions and was calculated according to the stoichiometry:

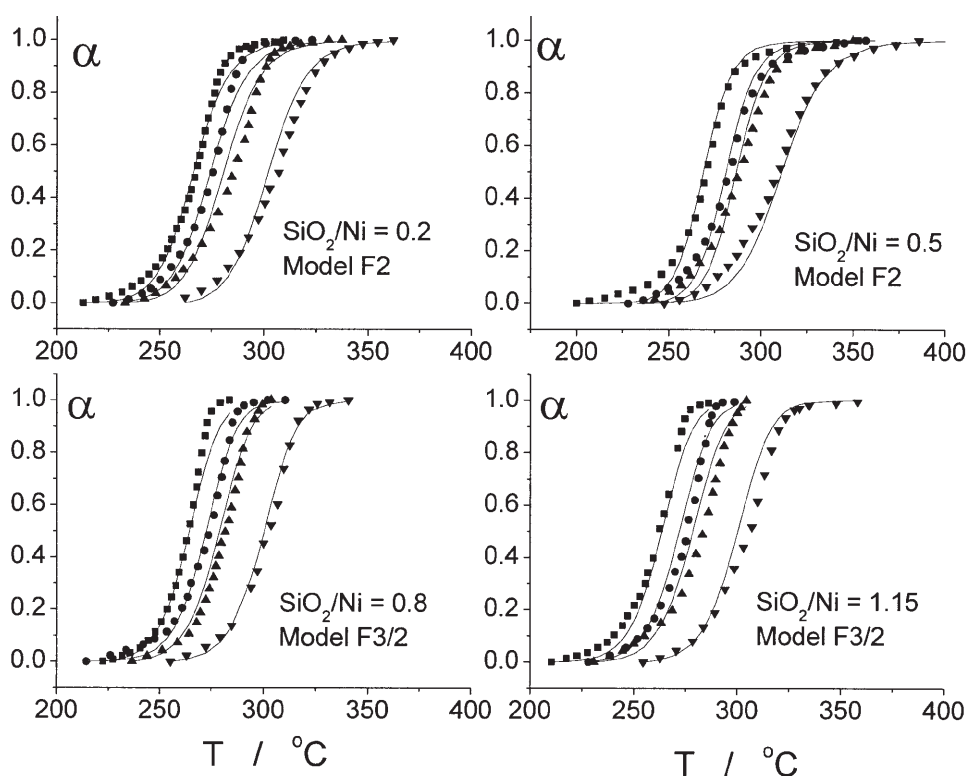
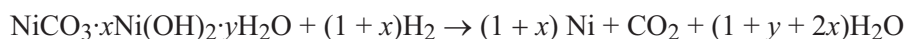


Fig. 1. Thermogravimetry results. The relative weight loss is presented as a function of temperature for all samples at all the applied heating rates. (Model abbreviations are explained in Table I. The lines are numerically simulated data and the symbols correspond to the experimental curves (■  $-\beta = 2^\circ/\text{min}$ ; ●  $-\beta = 5^\circ/\text{min}$ ; ▲  $-\beta = 10^\circ/\text{min}$ ; ▼  $-\beta = 20^\circ/\text{min}$ ).

The precursor composition is expressed through the stoichiometric coefficients  $x$  and  $y$  in a general formula of the form  $\text{NiCO}_3 \cdot x\text{Ni}(\text{OH})_2 \cdot y\text{H}_2\text{O}$  (Table II). According to these results, the stoichiometric coefficients  $x$  and  $y$  both increase with increasing  $\text{SiO}_2/\text{Ni}$  mole ratio. However, more experimental measurements would be needed to characterize the composition of the precursor samples better.

Nevertheless, the results of the TG were analyzed in their normalized form, by the multi-thermal history model-fitting method with non-linear regression.

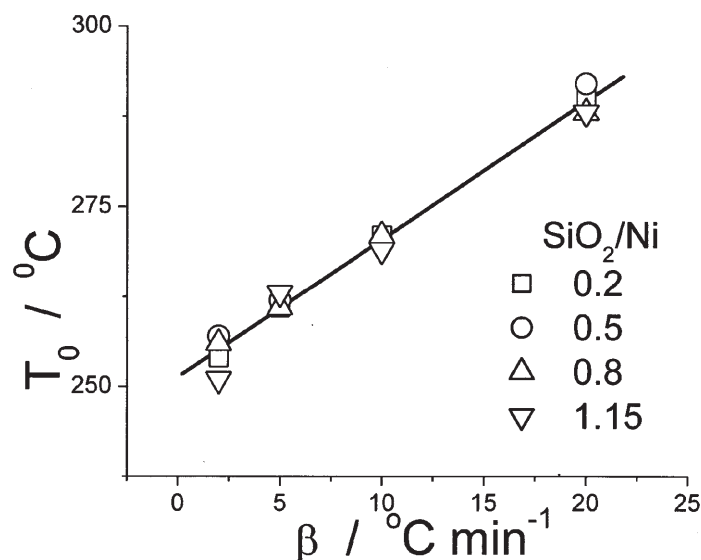


Fig. 2. The initial temperature of the transformation at different heating rates.

Therefore, the results of the kinetic analysis does not depend on any assumed stoichiometry. All of the models from Table I were tested to identify the reaction mechanism fitting the best. The Runge–Kutta algorithm was used for the integration of the differential equations and the simplex method was used for the minimization of the function to determine the optimal set of the parameters.<sup>18</sup> The mean sum of the squares of the residuals was used as the criterion function for the minimization process. Temperature centering was used to improve the robustness of the fitting procedure.<sup>17</sup>

TABLE II. The relative weight loss of the samples with given  $\text{SiO}_2/\text{Ni}$  mole ratio and calculated precursor composition according to the general formula of basic nickel carbonate  $\text{NiCO}_3 \cdot x\text{Ni}(\text{OH})_2 \cdot y\text{H}_2\text{O}$

Mole ratio $\text{SiO}_2/\text{Ni}$	$\Delta w/w$	$x$	$y$
0.2	0.47	0.47	2.07
0.5	0.39	0.70	2.23
0.8	0.32	0.85	2.76
1.15	0.27	1.26	3.20

The best fitting kinetic parameters obtained from the non-linear regression are presented in Table III for separate samples with given  $\text{SiO}_2/\text{Ni}$  ratios.

The simulations of the TG experiments with the optimal set of the parameters is, in general, well in accordance with the experimental data (lines on Fig. 1). However, it is obvious that the present model is not able to give a perfect match between the experimental and fitted results and more complex models with several reaction steps would probably lead to further improvement of the fitting. However, the obtained fitting was good enough to enable a choice between the models to be made.

TABLE III. Estimates of the kinetic parameters  $E_a$  and  $A$  for the samples with given  $\text{SiO}_2/\text{Ni}$  ratios and the sensitivity of the model (or of the fitting criterion function  $RSS$ ) against the parameters

$\text{SiO}_2/\text{Ni}$	Model	$E_a/\text{J mol}^{-1}$	$A/\text{min}^{-1}$	$\log(A)$	$RSS/f$	$S(E_a)/\%$	$S(A)/\%$
0.2	F2	2.67E+05	1.7E+25	25.2	2.3E-03	9	11
0.5	F2	3.04E+05	5.4E+28	28.7	8.4E-03	2	10
0.8	F3/2	2.65E+05	1.1E+25	25.0	2.5E-03	13	9
1.15	F3/2	2.56E+05	1.5E+24	24.2	4.8E+03	6	13
1.15	F2	2.41E+05	5.7E+22	22.8	4.5E-03	5	1

The variances ( $RSS/f$ ) depicting the goodness of fit and the sensitivities of the  $RSS$  criterion function to small (5 %) changes in the kinetic parameters  $S(E_a)$  and  $S(A)$  are also given in Table III. The sensitivities are expressed as the relative change in the  $RSS/f$  criterion function produced by a 5 % change in the kinetic parameters. The low values obtained for the variances are indication that a relatively good fit was achieved. The worst result was obtained for the sample with a  $\text{SiO}_2/\text{Ni}$  mole ratio of 0.5, but the corresponding variance was still lower than 0.01. On the other hand, the high values for the parametric sensitivities are an indication that the obtained values of the kinetic parameters are really optimal for the given experimental results and the chosen models.

Hence, the  $F$ -test was performed to discriminate between the various models and the results are presented in Table IV. In the bottom row of Table IV, the critical value of  $F_{95}$  was given for each sample. According to the performed  $F$ -test, the correct model could be chosen immediately for the samples with  $\text{SiO}_2/\text{Ni}$  mole ratio 0.2, 0.5 and 0.8 (F2 for the first two and F3/2 for the third one), but for the sample with a  $\text{SiO}_2/\text{Ni}$  mole ratio of 1.15 the two models fit equally well (F2 and F3/2).

TABLE IV. The results of the  $F$ -test for all samples and all models. The critical value  $F_{95}$  is shown in the bottom row. The results were compared for multiple TG curves obtained at different heating rates

	$\text{SiO}_2/\text{Ni}=0.2$	$\text{SiO}_2/\text{Ni}=0.5$	$\text{SiO}_2/\text{Ni}=0.8$	$\text{SiO}_2/\text{Ni}=1.15$
$F(R2)$	11.0	5.2	9.8	5.4
$F(R3)$	9.3	5.0	5.0	4.4
$F(F1)$	6.3	3.6	2.3	2.6
$F(F3/2)$	2.5	2.1	1.0	1.1
$F(F2)$	1.0	1.0	2.0	1.0
$F(A2)$	6.1	2.8	2.9	1.8
$F(A3)$	9.7	2.9	12.4	4.2
$F(A4)$	17.6	5.4	26.0	9.9
$F(D3)$	16.6	6.3	15.5	9.3
$F(D5)$	10.0	4.5	8.4	5.5
$F_{95}$	1.4	1.4	1.4	1.4



Therefore, either of the two best model can be arbitrarily chosen for the sample with a  $\text{SiO}_2/\text{Ni}$  mole ratio of 1.15. It is only easier to understand the change in the mechanism if the F3/2 model is chosen. If this model is the one that dominates for the sample with the highest  $\text{SiO}_2/\text{Ni}$  mole ratio, then it can be said that increasing the  $\text{SiO}_2/\text{Ni}$  mole ratio leads to a change in the reaction mechanism of the nickel reduction, resulting finally in a change from second order reaction kinetics to three halves order reaction kinetics.

As a result of the changes in the reaction mechanism, the activation energies and pre-exponential factors in the Arrhenius equation also changed. Moreover, the observed changes in the values of the kinetic parameters probably indicate that both mechanisms are competing during the reduction of all the samples. Therefore, increasing the  $\text{SiO}_2/\text{Ni}$  mole ratio leads to an increase in the contribution of F3/2 to kinetics of the overall reaction, relative to the contribution of F2.

The F2 kinetics are typical for phase boundaries reactions. However, the occurrence of F3/2 reaction kinetics can possibly be connected with branching mechanisms. It previously claimed that the thermal reduction of nickel oxide can be an autocatalytic process with a Ni metal intermediary product acting as a catalyst for the reduction itself.<sup>19</sup> This intermediary product may undergo sintering and grain growth leading to decreased activity and deceleration of the reaction. A similar process can be the cause of the observed F3/2 kinetics in the present case.

If two reaction mechanisms correspond to consecutive steps, then the overall kinetics correspond to the limiting, slowest step. For the samples with high  $\text{SiO}_2/\text{Ni}$  mole ratios (low nickel loading), it was found that the branching mechanism of the autocatalytic process of the metallic nickel particles is the limiting step. On the other hand, for the samples with a low  $\text{SiO}_2/\text{Ni}$  mole ratio (high nickel loading), the same process is no longer the limiting step, and reaction kinetics follow the second order rate law, typical for reactions on the phase boundaries.

As it was reported before,<sup>1</sup> the catalytic activity in soybean oil hydrogenation was also decreased for the corresponding samples with a high  $\text{SiO}_2/\text{Ni}$  mole ratio. The cause of the observed decrease in the catalytic activity with increasing  $\text{SiO}_2/\text{Ni}$  mole ratio could lie in the changes of the reaction mechanism of the Ni reduction. These results could be correlated with the results of other authors, who claimed that lower Ni loadings could be favourable for silicate formation, which was further connected with a lower reducibility.<sup>3</sup> The present results indicate that the catalyst properties could be affected by a slower grain formation process during the reduction in samples with a lower nickel loading.

#### CONCLUSION

A series of Ni catalyst precursors were synthesized with different  $\text{SiO}_2/\text{Ni}$  mole ratios, between 0.2 and 1.15. The reduction of all the prepared samples was studied by thermogravimetry at different heating rates between 2 and 20 degrees/min, in a

hydrogen flow. The final weight loss depends on the SiO<sub>2</sub>/Ni mole ratio but does not depend on the heating rate (Table II), indicating that complete hydrogenation was achieved with all samples.

The TG results were analyzed by the multi-thermal history model-fitting method with non-linear regression. The ten models given in Table I were tested to identify the reaction mechanism best fitting the obtained results. The best fitting kinetic parameters obtained from the non-linear regression were chosen according to the variance which depicts the goodness of the fit. The *F*-test was performed to discriminate between the various models. According to the *F*-test performed, for samples with a SiO<sub>2</sub>/Ni mole ratios 0.2 and 0.5, F2 is preferred and for samples with a SiO<sub>2</sub>/Ni mole ratio of 0.8, F3/2 is preferred. For the sample with a SiO<sub>2</sub>/Ni mole ratio of 1.15, both models are equally good. The F3/2 model was chosen for the last sample, because it makes it easier to understand and discuss the change in the mechanism.

Thus, increasing the SiO<sub>2</sub>/Ni mole ratio leads to a change in the reaction mechanism of the nickel reduction, resulting finally in a change from second order reaction kinetics to three halves order reaction kinetics. These results indicate a change in the rate limiting step, from autocatalytic grain growth for lower nickel loadings, to reaction on the phase boundaries for high nickel loadings.

*Acknowledgement:* This work was financed by the Ministry of Science, Technology and Development of Serbia under grant numbers HE\_1807 and MHT.2.09.0022.B.

#### ИЗВОД

#### НЕИЗОТЕРМАЛНА КИНЕТИЧКА КАРАКТЕРИЗАЦИЈА РЕАКЦИЈА ГАСНИХ И ЧВРСТИХ РЕАКТАНАТА TG АНАЛИЗОМ

ЖЕЉКО ЧУПИЋ,<sup>1\*</sup> ДУШАН ЈОВАНОВИЋ,<sup>1</sup> ЈУГОСЛАВ КРСТИЋ,<sup>1</sup> НИКОЛА ВУКЕЛИЋ<sup>2</sup> и  
ЗОРАН НЕДИЋ<sup>2</sup>

<sup>1</sup> Институт за хемију, технологију и металургију, Центар за катализу и хемијско инжењерство, Њеђосева 12, 11000 Београд и <sup>2</sup> Факултет за физичку хемију, Универзитет у Београду, П. бр. 137, 11001 Београд

Низ прекурсора Ni катализатора, на силикатном носачу је синтетисан са различитим SiO<sub>2</sub>/Ni молским односима, између 0,2 и 1,15. Редукција свих припремљених узорака је проучавана термогравиметријски (TG) у протоку водоника. На резултате TG анализа је примењена „метода фитовања моделима из вишеструке термалне историје“ са нелинеарном регресијом. Енергије активација су одређене за процес редукције на свим узорцима. Статистички *F*-тест је коришћен за дискриминацију међу моделима. Нађено је да повећање SiO<sub>2</sub>/Ni молског односа води промени реакционог механизма редукције Ni, што на крају доводи до промене кинетике од реакције другог реда до реакције реда 3/2.

(Примљено 9. јула 2004)

#### REFERENCES

1. D. Jovanović, R. Radović, Lj. Mareš, M. Stanković, B. Marković, *Cat. Today* **43** (1998) 21
2. M. Nele, A. Vidal, D. L. Bhering, J. C. Pinto, V. M. M. Salim, *Appl. Catal. A: General* **178** (1999) 177

3. D. L. Bhering, M. Nele, J. C. Pinto, V. M. M. Salim, *Appl. Catal. A: General* **178** (1999) 177
4. C. Duval, *Inorganic Thermogravimetric Analysis*, Elsevir Publishing Company, Amsterdam – London – New York, 1963, p. 361
5. Yan Wang, Jia-Jun Ke, *Materials Research Bulletin*, **31** (1996) 55
6. N. B. Singh, A. K. Ojha, *Thermochim. Acta* **378** (2001) 87
7. P. Burattin, M. Che, C. Louis, *J. Phys. Chem. B.* **101** (1997) 7060
8. R. R. Keuleers, J. F. Janssens, H. O. Desseyn, *Thermochim. Acta* **385** (2002) 127
9. J. J. M. Orfao, F. G. Martins, *Thermochim. Acta* **390** (2002) 195
10. A. K. Burnham, *Thermochim. Acta* **355** (2000) 165
11. S. Vyazovkin, C. A. Wight, *Thermochim. Acta* **340-341** (1999) 53
12. T. Ozawa, *Bull. Chem. Soc. Jpn.* **38** (1965) 1881
13. J. R. Opfermann, E. Kaiserberger, H. J. Flammersheim, *Thermochim. Acta* **391** (2002) 119
14. B. Roduit, *Thermochim. Acta* **355** (2000) 171
15. J. R. Opfermann, W. Hadrach, *Thermochim. Acta* **263** (1995) 29
16. B. Roduit, M. Maciejewski, A. Baiker, *Thermochim. Acta* **282/283** (1996) 101
17. B. W. Wojciechowski, N. M. Rice, *Experimental Methods in Kinetic Studies*, Revised Edition, Elsevier, Amsterdam, 2003, p. 62
18. D. Jovanović, Ž. Čupić, M. Stanković, Lj. Rožić, B. Marković, *J. Mol. Catal. A: Chemical* **159** (2000) 353
19. S. B. Jagtap, B. B. Kale, A. N. Gokarn, *Metallurg. Trans. B - Process Metallurgy*, **23** (1992) 93.